Journal of Advances in Medical and Biomedical Research | ISSN:2676-6264

Green-Synthesized Silver Nanoparticles from Sinapis alba Reprogram Apoptosis and Cell Survival Signaling in Esophageal Cancer Cells

Zahraa Q.A. Al-Ghalibi [1*], Ali A. A. Al-Ali [2], Hasna A.M. Mohaus [1]

1. *Department of Biology,College of Education- Qurna, University of Basrah, Iraq*
2. *College of Education for Pure Sciences, University of Basrah, Iraq*

Article Info

10.22034/JAMBR.34.4.7555.1

Received: 2026/06/27;

Accepted: 2026/08/10;

Published Online: 2026/08/23;

***Corresponding author:**

Zahraa Q.A. Al-Ghalibi,

Department of Biology,College of Education- Qurna, University of Basrah, Iraq

Email: zahraaqusay355@gmail.com

How to Cite This Article:

Al-Ghalibi Z, A.A.Al.Ali A, A.M. Mohaus H. Green-Synthesized Silver Nanoparticles from Sinapis alba Reprogram Apoptosis and Cell Survival Signaling in Esophageal Cancer Cells. J Adv Med Biomed Res 2026; 34(4):401-411.

ABSTRACT

Background & Objective: Esophageal cancer is an aggressive malignancy characterized by a poor prognosis and limited response to conventional therapies. This study evaluated the *in vitro* anticancer activity of silver nanoparticles (AgNPs) biosynthesized using the aqueous seed extract of *Sinapis alba* against the human esophageal cancer cell line SKGT-4, in comparison with the human non-cancerous epithelial cell line HBL-100.

Materials & Methods: AgNPs were synthesized from a 1 mM AgNO3 solution and characterized via UV–Vis, XRD, SEM, TEM, EDX, zeta potential, and FTIR analyses. Cytotoxicity, cell migration, apoptosis, and the relative expression of Caspase-8 and Caspase-9 were assessed using cell viability assays, migration assays, AO/EB staining, and RT-qPCR, respectively.

Results: The AgNPs were spherical to quasi-spherical, with particle sizes of 40–50 nm (SEM) and 10–30 nm (TEM). UV–Vis spectroscopy revealed a characteristic absorption peak at 430 nm, XRD confirmed a face-centered cubic (FCC) structure, EDX showed a silver content of 71.1%, and the zeta potential (–31.4 mV) indicated favorable colloidal stability. The AgNPs significantly inhibited SKGT-4 cell growth in a concentration- and time-dependent manner, achieving approximately 87% inhibition after 72 h with an IC_{50} of 220 µg/mL, compared with 456 µg/mL for HBL-100 cells. Furthermore, they inhibited cell migration, promoted apoptosis, significantly upregulated Caspase-8, and maintained Caspase-9 expression near control levels.

Conclusion: *Sinapis alba*-derived AgNPs exhibited selective *in vitro* anticancer activity against esophageal cancer cells by inhibiting proliferation and migration while promoting apoptosis, highlighting their potential as promising therapeutic candidates.

Keywords: *Silver nanoparticles, SKGT-4 cells, Apoptosis, Cell migration, Gene expression*

Copyright © 2026, This is an original open-access article distributed under the terms of the Creative Commons Attribution-noncommercial 4.0 International License which permits copy and redistribution of the material just in noncommercial usages with proper citation.

1. Introduction

Nanoparticles represent a breakthrough in nanotechnology, typically ranging from 1 to 100 nm in size and possessing a high surface area-to-volume ratio that enhances their interactions with biological systems. Among these, silver nanoparticles have gained considerable attention due to their chemical stability, catalytic and electrical properties, and potent antibacterial, antifungal, and antioxidant activities (1). Conventional methods for nanoparticle synthesis typically rely on physical and chemical approaches that often involve hazardous reagents, complex or energy-intensive procedures, and significant environmental risks (2). Consequently, green synthesis has emerged as a safer and eco-friendlier alternative, utilizing plant extracts or microorganisms as natural sources of biomolecules capable of reducing metal ions and stabilizing nanoparticles. Various plant extracts have been successfully employed to synthesize silver nanoparticles with diverse sizes, morphologies, and biological properties, including promising anticancer activity (2). Cancer remains a major global health challenge characterized by uncontrolled cell proliferation, tissue invasion, and metastasis (3). Esophageal cancer is a highly malignant disease associated with high mortality and frequent late-stage diagnosis. Its development is strongly associated with various risk factors, including smoking, alcohol consumption, gastroesophageal reflux, as well as genetic and dietary factors (4). Despite available treatments, therapeutic responses remain limited in many cases, highlighting an urgent need for alternative

approaches such as nanoparticle-based therapies. However, the anticancer effects of silver nanoparticles synthesized from yellow mustard (*Sinapis alba*) seed extract against human esophageal cancer, particularly SKGT-4 cells, remain insufficiently investigated. Therefore, this study aimed to synthesize silver nanoparticles using *S. alba* seed extract and evaluate their anticancer efficacy against esophageal cancer cells, with a particular focus on apoptosis and cell proliferation-related responses (5).

2. Materials and Methods

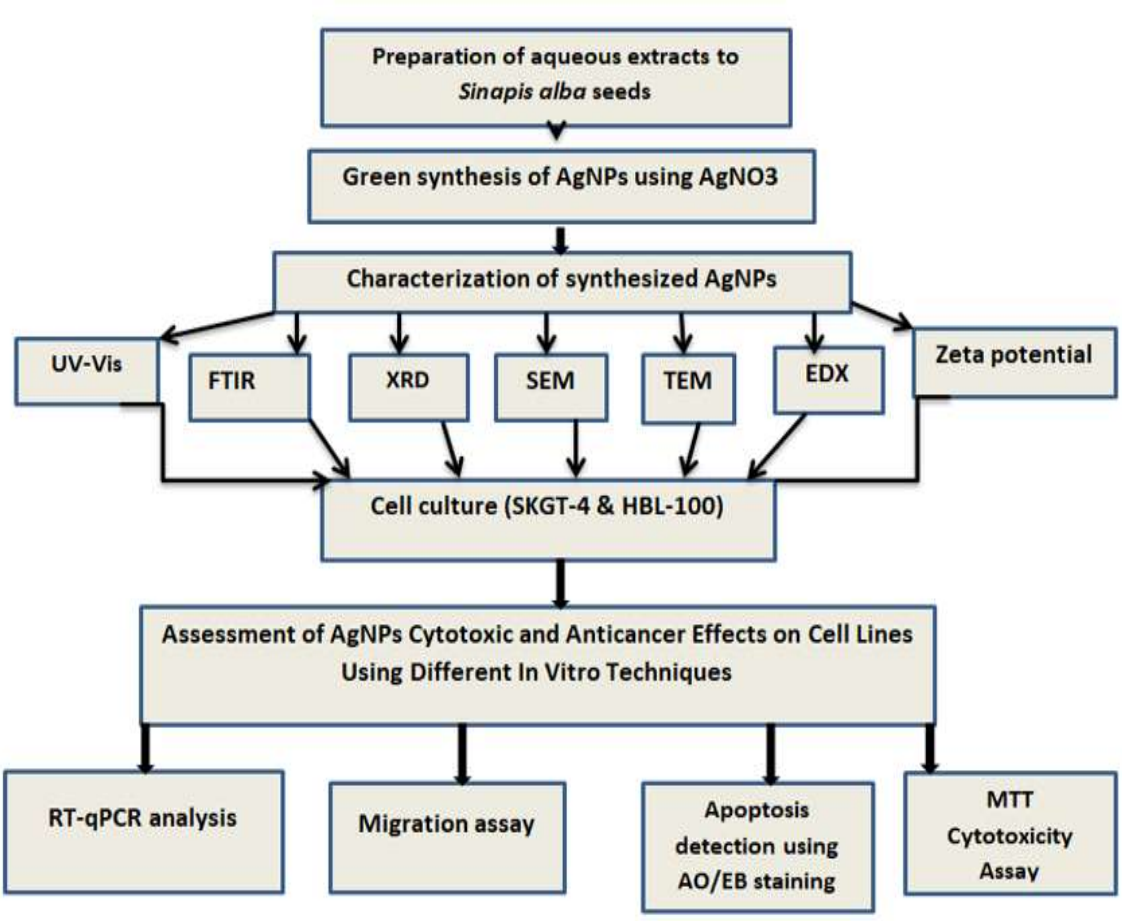


Figure 1. Main workflow of the study. (**Prepared by Authors, 2026**).

2.1 Preparation and Characterization of Silver Nanoparticles

Sinapis alba seeds were thoroughly washed, dried, and ground into a fine powder. The plant extract was prepared by heating 10 g of the powder in 100 mL of deionized water at 60 °C for 30 min, followed by filtration through Whatman No. 1 filter paper (Cytiva, USA). Silver nanoparticles were then synthesized by 90 mL of 1 mM $AgNO_3$ solution (Merck, Germany; Cat. No. 1.01512.0100) under continuous stirring at 60 °C until the solution color changed from light yellow to dark brown (6).

The synthesized AgNPs were characterized using UV–Vis spectrophotometry (200–1000 nm), FTIR spectroscopy (4000–400 cm−1), SEM, TEM, XRD, EDX spectroscopy, and zeta potential analyses. We adapted the synthesis protocol from previous work by the authors in the Basrah Journal of Science and fully detailed it here to ensure reproducibility (7).

2.2 Preparation of reagents and maintenance of cell lines

Complete RPMI-1640 medium (Capricorn Scientific, Germany/Korea) was supplemented with 10% FBS, sodium bicarbonate, and antibiotics (100 U/mL penicillin and 100 µg/mL streptomycin). The medium was sterilized by passage through a 0.22 µm syringe filter and stored at 4 °C. Serum-free RPMI-1640, PBS (Thermo Fisher Scientific, USA), Trypsin–Versene (Capricorn Scientific), 3-(4,5-dimethylthiazol-2-yl)-2,5-diphenyltetrazolium bromide (MTT; 5 mg/mL), and acridine orange/ethidium bromide (AO/EB) staining solutions (Scharlab, Spain) were prepared and maintained

according to standard laboratory protocols (8). The biosynthesized AgNPs were serially diluted in serum-free medium to achieve concentrations ranging from 62.5 to1000 µg/mL. SKGT-4 human esophageal adenocarcinoma cells and HBL-100 non-cancerous epithelial cells, obtained from the Cancer Research Cell Bank (University of Basrah), were cultured in complete RPMI-1640 medium at 37 °C in a humidified atmosphere containing 5% CO_2. Cells were subcultured at 80–90% confluence following standard trypsinization procedures.

2.3 Evaluation of Nanoparticale Cytotoxicity Using the MTT Assay

For the MTT assay, cells were seeded in 96-well flat-bottom plates at a density of 1 × 10^4 cells/well in 100 µL of complete RPMI-1640 medium and incubated for 24 h at 37 °C in 5% CO2. Following initial attachment, cells were treated with *Sinapis alba*-derived AgNPs at concentrations of 62.5, 125, 250, 500, and 1000 µg/mL in serum-free medium (with three replicates per concentration, alongside an untreated control group) and incubated for 72 h. Subsequently, 10 µL of MTT solution (5 mg/mL) was added to each well along with 90 µL of serum-free medium, and the plates were incubated for 2 h. After carefully aspirating the medium, 100 µL of dimethyl sulfoxide (DMSO) was added to dissolve the resulting formazan crystals (9). Absorbance was measured at 620 nm using a microplate reader (Thermo Fisher Scientific, USA). Cell growth inhibition was calculated relative to the untreated control group, and the half-maximal inhibitory concentration (IC_{50}) values for both SKGT-4 and HBL-100 cells were determined from dose–response curves using GraphPad Prism (version 10.1) based on three independent biological replicates (10).

2.4 Detection of Cell Death Using Acridine Orange/Ethidium Bromide Staining

Following 48 h of treatment with the IC_{50} concentration of the synthesized AgNPs, cells cultured on 8-well chamber slides were gently washed with phosphate-buffered saline (PBS) and stained with 20 µL of an acridine orange/ethidium bromide (AO/EB) dual-staining solution (100 µg/mL for each dye). The slides were immediately examined using a fluorescence microscope (MICROS, Austria). Viable cells exhibited uniform green fluorescence, early apoptotic cells displayed bright green nuclei with chromatin condensation (orange/yellow-orange), and late apoptotic or necrotic cells appeared red. Quantitative image analysis was performed using ImageJ software (NIH, version 1.53t), where cells in each category were counted and expressed as a percentage relative to the control group. The excitation/emission (Ex/Em) wavelengths for AO and EB fluorescence detection were set at approximately 500/526 nm and 520/590 nm, respectively (10,11).

2.5 Transwell migration assay

For the Transwell migration assay, cells were resuspended in RPMI-1640 medium containing 10% FBS at a density of 1×10^6cells/mL, and 100 µL of the cell suspension was added to the upper chamber of 8-µm-pore polycarbonate membrane inserts (Nest).

The lower chamber was filled with 600 µL of complete medium containing 10% FBS to establish a chemotactic gradient.

After incubation for 24 h at 37 °C in 5% CO_2, cells were treated with the IC_{35} concentration of AgNPs (154.4 µg/mL)" (established as a sub-cytotoxic concentration for evaluating migration inhibition), with untreated cells serving as the control group. Following incubation, non-migrated cells on the upper surface of the membrane were gently removed using a cotton swab.

Migrated cells on the lower surface were fixed with 70% ethanol for 10 min, stained with 0.2% Crystal Violet (Capricorn Scientific, Korea) for 5–10 min, and thoroughly washed with distilled water. To quantify migration, the bound stain was eluted with acetic acid, and the absorbance was measured at 450 nm using a microplate reader; staining intensity was additionally verified and quantified using ImageJ software. The migration of the untreated control group was set as 100% (12).

2.6 Study of Gene Expression of Programmed Cell Death Genes and Proliferative Genes

For gene expression analysis, cells were seeded at 2 × 10^6 cells/dish in 5 mL complete RPMI-1640 medium and incubated for 24 h at 37°C and 5% CO_2. Cells were then treated with the IC_{50} concentration of AgNPs for 24 h, with three biological replicates and an untreated control. Total RNA was extracted using the GEBEzol TriRNA Pure Kit (GEBEzol™, Taiwan; Cat. No. GZR100) according to the manufacturer's instructions, treated with DNase I, and quantified using a NanoDrop device.

cDNA was synthesized using Oligo(dT) in a final volume of 20 µL. qPCR was performed in 25 µL reactions containing 12.5 µL GoTaq® qPCR Master Mix, 1 µL each of forward and reverse primers, 5 µL cDNA, and 5.5 µL nuclease-free water. The thermal profile consisted of 95°C for 2 min, followed by 45 cycles of 95°C for 30 s, 60°C for 30 s, and 72°C for 30 s, with a final extension at 72°C for 10 min.

Each biological replicate was analyzed using four technical replicates, and mean biological-replicate values were used for statistical analysis. Primer sequences for the target genes are presented in Table 1.

Table 1. Target genes with their primers sequences.

Target gene	Sequence (5′–3′)	Length (bp)	GC (%)	Tm (°C)	Ref
Caspase 8-F	5-CATCCAGTCACTTTGCCAGA-3	20	50.0	60	(13)
Caspase 8-R	5-GCATCTGTTTCCCCATGTTT-3	20	50.0	60	
Caspase 9-F	5-GTTTGAGGACCTTCGACCAGCT-3	22	59.1	68	(13)
Caspase 9-R	5-CAACGTACCAGGAGCCACTCTT-3	22	59.1	68	
PIK3CA_F	5'_GGTTGTCTGTCAATCGGTGT_3'	20	55.0	62	(14)
PIK3CA_R	5'_GAACTGCAGTGCACCTTTCAAGC_3'	23	56.5	70	
AKT1_F	5'_TTCTGCAGCTATGCGAATGTG_3'	21	52.4	62	(14)
AKT1_R	5'_TGGCCAGCATACCATAGTGAGGTT_3'	24	58.3	72	
MTOR_F	5'_GCTTGATTTGGTTCCCAGGACAGT_3'	24	58.3	72	(14)
MTOR_R	5'_GTGCTGAGTTTGCTGTACCCATGT_3'	24	58.3	72	
GAPDH_F	5'__TGCACCACCAACTGCTTAGC_3'	20	60.0	62	(14)
GAPDH_R	5'_GGCATGGACTGTGTGGTCATGAG_3'	23	65.2	74	

The expression levels of the target genes were evaluated using the CT values and normalized to the reference gene by calculating ΔCT and ΔΔCT values. Relative gene expression was determined using the $2^{-\Delta\Delta CT}$ method to compare the control and treated groups.

2.7 Statistical Analysis

Statistical analysis was performed using GraphPad Prism 10.1. Data were expressed as mean ± SD. One-way ANOVA and Student's t-test were used for group and pairwise comparisons, respectively. IC_{50} values were determined from dose–response curves using nonlinear regression. Statistical significance was set at $P < 0.05$.

3. Result

3.1 Silver Nanoparticle Results

The biosynthesis of silver nanoparticles (AgNPs) using Sinapis alba seed extract was indicated by the color change of the reaction mixture from light yellow to reddish-brown at 60 °C (Figure 2A). UV–Vis analysis confirmed AgNP formation by showing a characteristic surface plasmon resonance (SPR) peak at 430 nm (Figure 2B). FTIR analysis revealed functional groups, including hydroxyl, amine, sulfur-containing, carbonyl, alkene, nitro, alkane, and C–O groups, which may contribute to the reduction and stabilization of the nanoparticles (Figure 2E).

SEM and TEM analyses showed predominantly spherical to quasi-spherical nanoparticles, with particle sizes of 40–50 nm and 9.68–29.12 nm, respectively (Figure 2C, D). XRD analysis confirmed the crystalline structure, with diffraction peaks at 27.84°, 32.24°, 38.16°, 46.28°, 54.90°, and 57.56°, corresponding to the (110), (111), (200), (211), (220), and (311) planes and matching Ag and Ag_2O reference patterns (Figure 2F). EDX analysis confirmed silver as the predominant element, with 71.1% atomic and 55.05% weight percentages (Figure 2G; Table 2). Zeta potential analysis showed a negative surface charge of −31.4±5.43 mV, indicating good colloidal stability (Figure 2H).

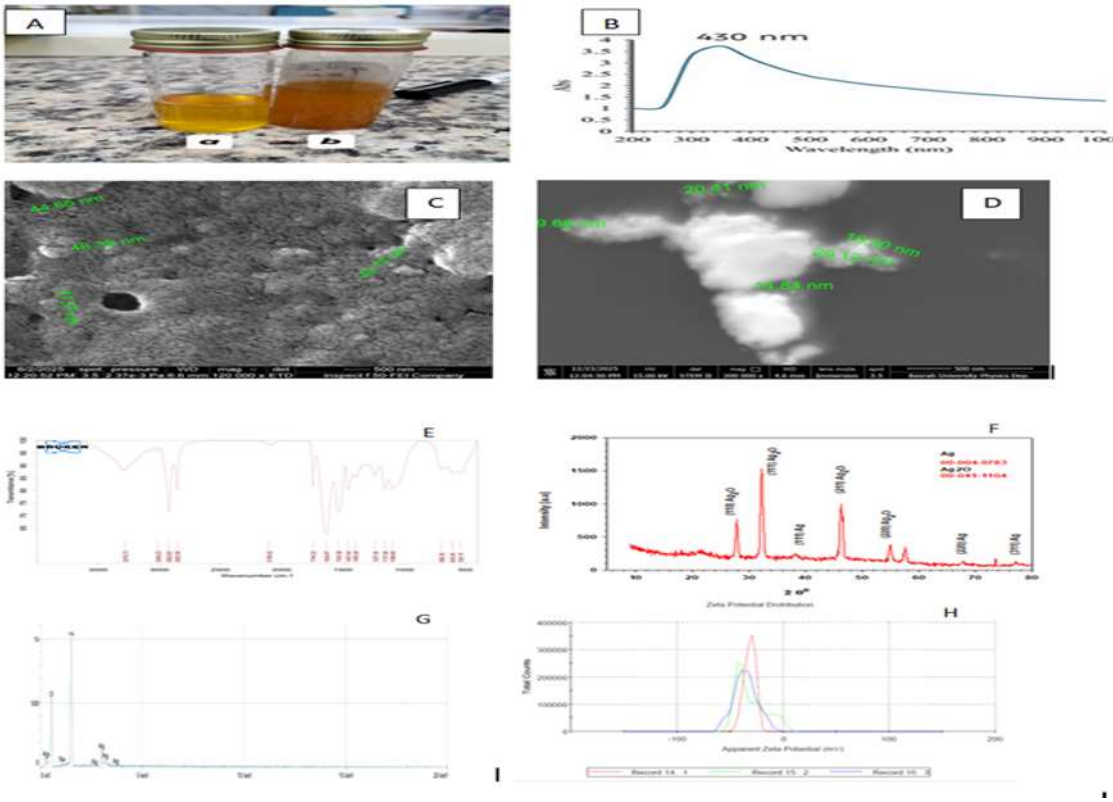


Figure 2. Characterization of Sinapis alba-derived AgNPs: (A) color change during synthesis; (B) UV–Vis absorption spectrum; © SEM and (D) TEM images; (E) FTIR spectrum; (F) XRD pattern; (G) EDX analysis; and (H) zeta potential. (**Prepared by Authors, 2026**).

Table 2. Elemental composition of Sinapis alba-derived AgNPs determined by EDX analysis.

Element	Atomic %	Weight %
Ag	71.1	55.0
Na	1.0	1.1
O	27.9	44.0

3.2 Cytotoxic Effect of Silver Nanoparticles

The MTT assay showed a dose-dependent inhibitory effect of *Sinapis alba*-derived AgNPs on SKGT-4 and HBL-100 cells after 72 h. In SKGT-4 cells (Figure 3B), inhibition increased from approximately 10% at 62.5 µg/mL to 87% at 1000 µg/mL, whereas inhibition in HBL-100 cells remained below 50% (Figure 3A). The IC_{50} values were approximately 220 µg/mL for SKGT-4 (Figure 3D) and 456 µg/mL for HBL-100 (Figure 3C), and these concentrations were subsequently used for the AO/EB and migration assays.

3.3 Cell Migration Assay

The Transwell assay showed a significant reduction in SKGT-4 cell migration after treatment with the IC_{35} concentration of Sinapis alba-derived AgNPs for 24 h (Figure 3E). Crystal Violet absorbance decreased from 1.22 ± 0.03 in the control to 0.75 ± 0.03 in treated cells, corresponding to 61.93% of control migration and 38.1% migration inhibition ($P < 0.05$). Microscopic images also supported the decrease in the number of migrating cells in the treated group (Figure 3F) compared with the untreated group (Figure 4G **).**

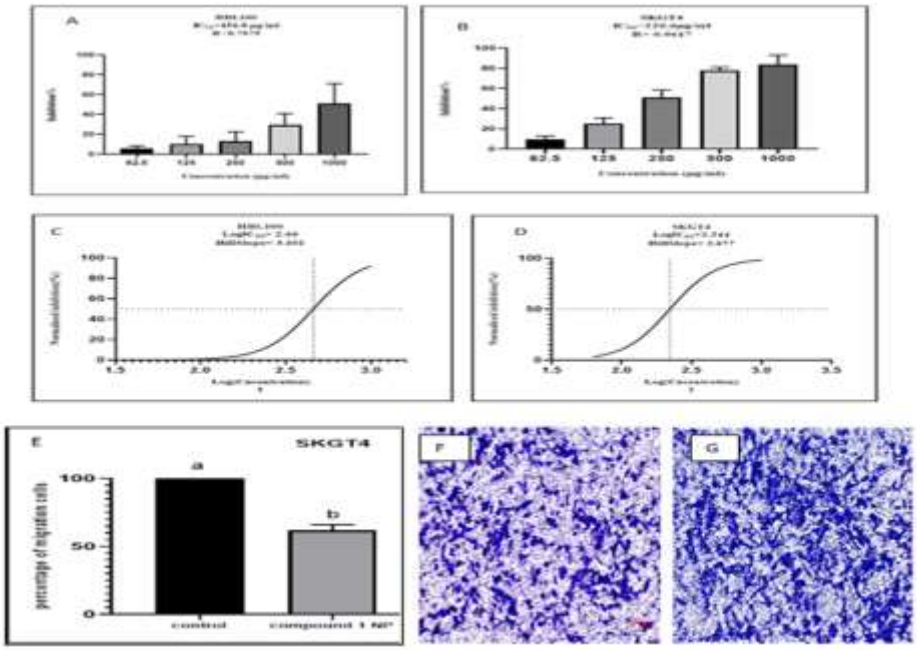


Figure 3. Cytotoxic and anti-migratory effects of Sinapis alba-derived AgNPs: (A, B) inhibition of HBL-100 and SKGT-4 cell growth, respectively, after 72 h; (C, D) dose–response curves and IC_{50} determination for HBL-100 and SKGT-4 cells, respectively; (E) SKGT-4 cell migration after 24 h; and (F, G) representative Transwell images of AgNP-treated and untreated cells, respectively. Different letters indicate significant differences ($P \leq 0.05$). **(Prepared by Authors, 2026)**.

3.4 Cell Death Detection with AO/EB

AO/EB staining showed predominantly green fluorescence with normal nuclei in untreated HBL-100 (Figure 4A) and SKGT-4 cells (Figure 4B), indicating high cell viability, whereas AgNP treatment for 48 h increased orange and red fluorescence, indicating apoptotic and dead cells. In HBL-100 cells (Figure 4C, E), viability decreased from 98% to approximately 68%, with about 17% early and 14% late apoptosis. In SKGT-4 cells, viability decreased from 98% to approximately 55%, with about 23% early and 20% late apoptosis (Figure 4D, F **).**

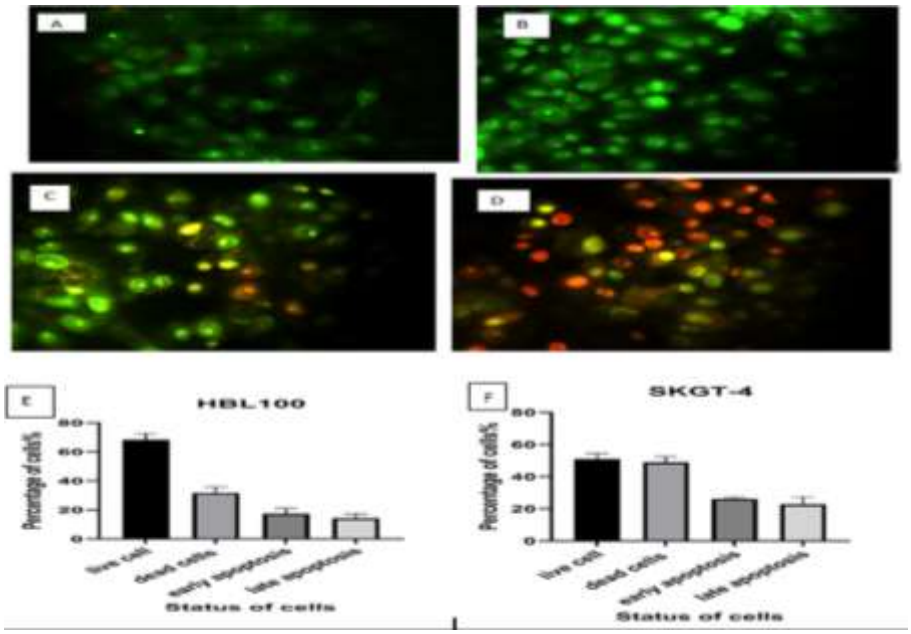


Figure 4. AO/EB fluorescence staining and quantitative analysis of apoptosis in HBL-100 and SKGT-4 cells after 48 h of treatment with AgNPs biosynthesized using Sinapis alba extract. (A, B) Untreated HBL-100 and SKGT-4 cells, respectively, as negative controls; (C, D) AgNP-treated HBL-100 and SKGT-4 cells, respectively. Viable cells exhibited uniform green fluorescence, early apoptotic cells appeared yellowish-green/yellow, and late apoptotic or necrotic cells showed orange-red fluorescence. (E, F) Quantitative analysis of apoptotic cell stages in HBL-100 and SKGT-4 cells, respectively. Images were captured using a fluorescence microscope equipped with appropriate AO/EB filters. **(Prepared by Authors, 2026)**.

3.5 Expression of Apoptotic Genes

RT-qPCR analysis showed altered expression of apoptotic genes in SKGT-4 cells treated with *Sinapis alba*-derived AgNPs. Caspase-8 expression increased to 3.32±1.68 corresponding to an approximately 232% increase (Figure 5A), whereas Caspase-9 expression decreased slightly to 0.74, representing an approximately 26% reduction (Figure 5B).

3.6 Expression of PI3K/AKT/mTOR Pathway Genes

RT-qPCR analysis showed increased expression of PI3K/AKT/mTOR pathway genes in SKGT-4 cells treated with *Sinapis alba* AgNPs. PI3K expression increased to 4.23 ± 0.98-fold (323%) (Figure 5, C), AKT1 to 1.90 ± 0.30-fold (90%) (Figure 5, D)., and mTOR to 2.83 ± 0.56-fold (183%) (Figure 5, E). compared with the control group.

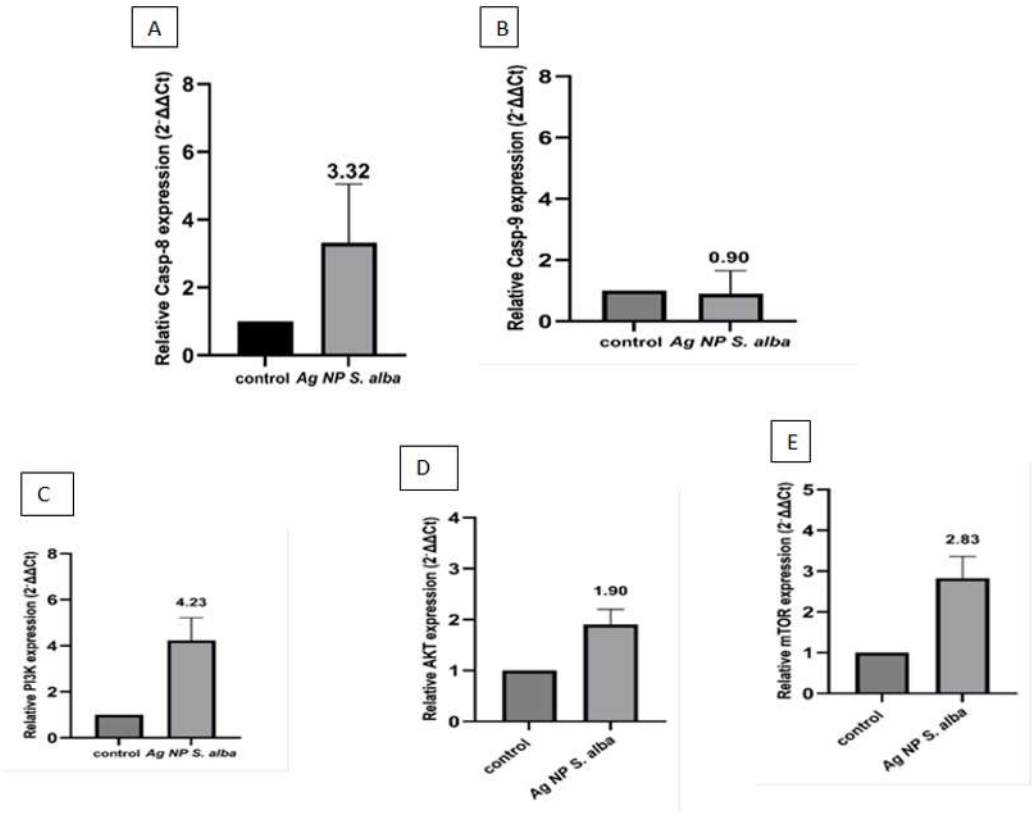


Figure 5. Relative expression levels of apoptosis- and PI3K/AKT/mTOR pathway-related genes in SKGT-4 cells treated with biosynthesized AgNPs from Sinapis alba at the IC_{50} concentration. (A) Caspase-8, (B) Caspase-9, (C) PI3K, (D) AKT1, and (E) mTOR relative expression levels compared with the untreated control group. Data are presented as mean ± SD from three biological replicates with four technical replicates. Statistical significance was determined using Student's t-test, with $P < 0.05$ considered significant. (**Prepared by Authors, 2026**).

4. Discussion

4.1 Discussion of AgNPs Synthesis Using *Sinapis alba* Extract

The successful biosynthesis of silver nanoparticles (AgNPs) using *Sinapis alba* seed extract was initially indicated by a color change in the reaction mixture from light yellow to reddish-brown, resulting from the reduction of Ag^+ to Ag^0 and the subsequent surface plasmon resonance (SPR). This reducing and stabilizing activity is primarily attributed to the bioactive compounds present in the extract, such as phenolics, flavonoids, proteins, and sulfur-containing compounds (6). UV–Vis analysis further confirmed AgNP formation through a characteristic SPR peak at 430 nm, indicating the production of relatively stable nanoparticles; this SPR band is influenced by particle size, morphology, and the surrounding chemical environment (15,16). FTIR analysis identified hydroxyl, carbonyl, amine, and sulfur-containing functional groups, supporting the involvement of plant phytochemicals in Ag^+ reduction and nanoparticle stabilization (16). SEM and TEM revealed predominantly spherical to quasi-spherical particles, with sizes of 40–50 nm and 9.68–29.12 nm, respectively; this discrepancy may be attributed to the distinct measurement principles of the two techniques and the presence of an organic phytochemical coating (17). XRD confirmed the crystalline nature and face-centered cubic (FCC) structure of the AgNPs, while the presence of some Ag_2O peaks may indicate partial surface oxidation during biosynthesis (16,18). EDX confirmed silver as the predominant element, with minor elements likely originating from residual plant-derived compounds, supporting the successful formation and relatively high purity of the

nanoparticles (13,14). Finally, the negative zeta potential (−31.4 ± 5.43 mV) and a narrow, single size distribution indicated good colloidal stability and a relatively uniform surface charge, likely due to the adsorption of phytochemicals onto the nanoparticle surface, which prevents aggregation (18,19).

4.2 Cytotoxic Effect

The present study demonstrated that *Sinapis alba*-mediated AgNPs exerted a concentration-dependent cytotoxic effect on SKGT-4 cells, with inhibition ranging from 10% to 87% after 72 h and an IC_{50} of approximately 220 µg/mL. In contrast, inhibition in HBL-100 cells remained below 50%, with a higher IC_{50} of approximately 456 µg/mL, suggesting that SKGT-4 cancer cells possess greater sensitivity to the treatment than HBL-100 cells (20). Since the MTT assay primarily reflects cellular metabolic activity, the observed reduction in viability may be attributed to impaired mitochondrial function, reduced proliferation, or the induction of programmed cell death (21). The cytotoxicity of AgNPs likely involves cellular uptake, interaction with intracellular components, and the induction of oxidative stress through ROS generation, which can subsequently activate apoptotic pathways (22). Although ROS levels were not directly quantified in this study, the observed morphological alterations and gene expression profiles support the potential involvement of oxidative stress in the cytotoxic response. These findings align with previous reports of the cytotoxic effects of biogenic AgNPs against various cancer cell lines, where activity is governed by cell type, nanoparticle characteristics, and the specific biological reducing agent used (23). Furthermore, the presence of plant-derived phytochemicals on the nanoparticle surface may enhance both biocompatibility and selective cytotoxicity; in particular, bioactive compounds from *S. alba*, such as isothiocyanates, may further augment their anticancer efficacy (24).

4.3 Inhibition of Cancer Cell Migration

The Transwell assay demonstrated that treatment with Sinapis alba AgNPs significantly reduced the migration of SKGT-4 esophageal cancer cells compared with the control, as indicated by the decreased crystal violet absorbance and the lower number of migrating cells observed microscopically (25). The assay was performed at a sub-cytotoxic concentration (IC_{35} = 154.4 µg/mL), reducing the possibility that the observed inhibition was solely due to decreased cell viability. These findings suggest that the AgNPs may interfere with cellular processes involved in cancer cell migration, supporting their potential anticancer activity.

4.4 Indicators of Cell Death

Acridine Orange/Ethidium Bromide (AO/EB) fluorescence staining was employed to differentiate between viable, apoptotic, and necrotic cells based on alterations in fluorescence emission and membrane integrity (26). Untreated HBL-100 and SKGT-4 cells exhibited predominantly green fluorescence with intact nuclei, signifying preserved membrane integrity and minimal cell death (27). Conversely, treatment with *Sinapis alba*-mediated AgNPs induced a distinct chromatic shift from green to orange/red fluorescence, corresponding to an increase in early apoptotic, late apoptotic, and necrotic cell populations in both cell lines. This pro-apoptotic effect is likely driven by AgNP-induced ROS generation and subsequent oxidative stress, which can compromise DNA, protein, and lipid integrity, thereby triggering apoptotic signaling pathways (28). Notably, SKGT-4 cells exhibited heightened sensitivity compared to HBL-100 cells, a phenomenon potentially attributable to their elevated metabolic activity and increased susceptibility to oxidative insult (29).

4.5 Regulation of Caspase-8 and Caspase-9 and the Compensatory PI3K/AKT/mTOR Response

RT-qPCR analysis showed increased Caspase-8 expression with only a slight decrease in Caspase-9 expression after treatment with *Sinapis alba* AgNPs, suggesting greater transcriptional involvement of the extrinsic apoptotic pathway under the present conditions (30). However, increased Caspase-8 expression alone does not confirm its functional activation, as caspases require proteolytic cleavage. Similarly, the slight change in Caspase-9 does not exclude mitochondrial involvement. Since ROS, mitochondrial function, and caspase protein activation were not assessed, these mechanisms remain preliminary. Both apoptotic pathways ultimately converge on Caspase-3, whose expression or activation was not evaluated; therefore, further protein-level studies are required to confirm downstream apoptosis.

The biological activity of Sinapis alba AgNPs may also be influenced by plant-derived compounds such as phenolics, flavonoids, and alkaloids, which can affect nanoparticle properties and their interactions with cells (31). In addition, PI3K, AKT, and mTOR expression increased following AgNP treatment. Since pathway activation depends mainly on protein phosphorylation, these transcriptional changes do not necessarily indicate functional activation of the PI3K/AKT/mTOR pathway (32). Rather, they may represent a compensatory survival response to treatment-induced cellular stress occurring alongside apoptotic signaling. Although this pathway can also interact with mitochondrial apoptotic mechanisms, the observed reduction in MTT activity confirms impaired cellular metabolic activity and viability despite the increased expression of survival-related genes (33). Overall, the findings provide preliminary evidence for transcriptional regulation of apoptotic and survival pathways, but confirmation using functional assays such as Annexin V/PI, caspase activity, cleaved Caspase-3/Caspase-8, and PARP cleavage is required (34).

5. Conclusion

This study demonstrated that silver nanoparticles (AgNPs) biosynthesized using aqueous *Sinapis alba* seed extract exerted a concentration-dependent anticancer effect against SKGT-4 cells, showing greater sensitivity compared to HBL-100 cells. The AgNPs also inhibited cell migration and induced apoptosis, as evidenced by AO/EB staining. Furthermore, the increased expression of

Caspase-8 provided preliminary evidence for the potential involvement of the extrinsic apoptotic pathway. Overall, these findings support the potential of *S. alba*-mediated AgNPs as anticancer agents; however, further *in vivo* and mechanistic studies are required to fully elucidate their therapeutic potential.

6. Declarations

6.1 Acknowledgments

The authors would like to express their sincere gratitude to Dr. Ali for his valuable assistance in cell culture and experimental procedures, and to Dr. Hasna for her continuous scientific support, guidance, and provision of references and research materials throughout the study. The authors also extend their appreciation to the laboratory staff for their technical support during the experimental work. Special thanks are due to everyone who contributed to the completion of this research.

6.2 Ethical Considerations

Ethical approval was not required for this study, as confirmed by the authors in a formal declaration.

6.3 Authors' Contributions

Zahraa Q. A. Al-Ghalibi contributed to the conceptualization, investigation, data collection, formal analysis, and writing of the original draft. Ali A. A. Al-Ali contributed to the supervision, methodology, and critical revision of the manuscript. Hasna A. M. Mahous contributed to the investigation, data interpretation, and revision of the manuscript. All authors reviewed and approved the final version of the manuscript.

6.4 Conflict of Interest

The authors declare no conflict of interest.

6.5 Fund or Financial Support

This research received no external funding.

6.6 Using Artificial Intelligence Tools (AI Tools)

Artificial intelligence (AI) tools were used to a very limited extent to assist in interpreting some data and identifying relevant references and websites. The authors reviewed and verified the information and take full responsibility for the content of the manuscript.

References

1. Srinivasan LV, Rana SS. A critical review of various synthesis methods of nanoparticles and their applications in biomedical, regenerative medicine, food packaging, and environment. Discover Appl Sci. 2024;6:371 [DOI:10.1007/s42452-024-06040-8]

2. Osman AI., Zhang Y, Farghali M, Rashwan AK, Eltaweil AS, Monaem A,et al. Synthesis of green nanoparticles for energy, biomedical, environmental, agricultural, and food applications: A review. Environment Chem Lett.2024; 22(2): 841-87. [DOI:10.1007/s10311-023-01682-3]

3. Turnquist C, Taylor TR, Al-Mossawi H, Watson RA. The principles of neoplasia and oncology. Surgery-Oxford International Edition.2024; 42(3):125-32.

[DOI:10.1016/j.mpsur.2023.12.002]

4. Ilic I, Zivanovic Macuzic I, Ravic-Nikolic A, Ilic M, Milicic V. Global burden of esophageal cancer and its risk factors: a systematic analysis of the global burden of disease study 2019. Life.2024; 15(1): 24. [DOI:10.3390/life15010024] [PMID] [PMCID]

5. Mitrović PM, Stamenković OS, Banković-Ilić I, Djalović IG, Nježić ZB, Farooq M,et al. White mustard (Sinapis alba L.) oil in biodiesel production: A review. Front Plant Sci.2020; 11, 299. [DOI:10.3389/fpls.2020.00299] [PMID] [PMCID]

6. 6- Alharbi NS, Khaled JM, Alanazi K, Kadaikunnan S, Alobaidi AS. Biosynthesis of silver nanoparticles (Ag-NPs) using Senna alexandrina grown in Saudi Arabia and their bioactivity against multidrug-resistant pathogens and cancer cells. Saudi Pharmaceut J.2023; 31(6): 911-20. [DOI:10.1016/j.jsps.2023.04.015] [PMID] [PMCID]

7. Al-Ghalibi ZQA, Al-Ali AA, Mahous HA. Green synthesis of environmentally friendly silver nanoparticles with Solanum melongena plant peels and Sinapis alba plant seeds extract. Accepted for publication in Basrah Journal of Science

8. Al-Ali AA, Alsalami KA, Athbi AM. Cytotoxic effects of CeO2 NPs and β-Carotene and their ability to induce apoptosis in human breast normal and cancer cell lines. Iraq J Sci.2022;923-37. [DOI:10.24996/ijs.2022.63.3.2]

9. Ullah I, Khalil AT, Ali M, Iqbal J, Ali W, Alarifi s,et al. Green-synthesized silver nanoparticles induced apoptotic cell death in MCF-7 breast cancer cells by generating reactive oxygen species and activating caspase 3 and 9 enzyme activities. Oxid Med Cell Longevit.2020; 2020(1): 1215395. [DOI:10.1155/2020/1215395] [PMID] [PMCID]

10. 10-Aghara H, Samanta S, Patel M, Chadha P, Patel D, Jha A, et al. (2025). Silver nanoparticles synthesized from Enicostemma littorale exhibit gut tight junction restoration and hepatoprotective activity via regulation of the inflammatory pathway. Pharmaceutics.2025; 17(7): 895.

[DOI:10.3390/pharmaceutics17070895] [PMID] [PMCID]

11. Paua JC. In vitro anticancer activity of Phyla nodiflora. Egypt Acad J Biol Sci B Zool. 2022;14:397-409. [DOI:10.21608/eajbsz.2022.274521]

12. Wang R, Zhong H, Wang C, Huang X, Huang A, Du N ,et al. Tumor malignancy by genetic transfer between cells forming cell-in-cell structures. Cell Death & Disease.2023; 14(3):195. [DOI:10.1038/s41419-023-05707-1] [PMID] [PMCID]

13. Falih SM, Al-Saray ST, Alfaris AA, Al-Ali AA. The synergistic effect of eucalyptus oil and retinoic acid on human esophagus cancer cell line SK-GT-4. Egyptian journal of medical human genetics.2022; 23(1):70. [DOI:10.1186/s43042-022-00259-z]

14. Al-Batat Zha. PI3K/AKT/mTOR pathway study. MSc Thesis, Univ Basrah. 2023.

15. Iwuji H Saha, Ghann W, Dotson D, Bhuiya K, Parvez M, et al., Synthesis and characterization of silver nanoparticles and their promising antimicrobial effects. Chem Phys Impact. 2024;9:100758

[DOI:10.1016/j.chphi.2024.100758]

16. Singh A, Sharma B, Deswal R. Green silver nanoparticles from novel Brassicaceae cultivars with enhanced antimicrobial potential than earlier reported Brassicaceae members. J Trace Element Med Biol .2018;47, 1-11 [DOI:10.1016/j.jtemb.2018.01.001] [PMID]

17. Demirel Bayik G, Baykal B. Impact of plant species on the synthesis and characterization of biogenic silver nanoparticles: A comparative study of brassica oleracea, Corylus avellana, and camellia sinensis. Nanomaterials.2024; 14(23): 1954. [DOI:10.3390/nano14231954] [PMID] [PMCID]

18. Somda D, Bargul JL, Wesonga JM, Wachira SW. Green synthesis of Brassica carinata microgreen silver nanoparticles, characterization, safety assessment, and antimicrobial activities. Sci Rep.2024;14(1): 29273.

[DOI:10.1038/s41598-024-80528-6] [PMID] [PMCID]

19. Ansar S, Tabassum H, Aladwan NS, Naiman Ali M, Almaarik B, AlMahrouqi S,et al.. Eco friendly silver nanoparticles synthesis by Brassica oleracea and its antibacterial, anticancer and antioxidant properties. Scientific Reports.2020; 10(1):18564. [DOI:10.1038/s41598-020-74371-8] [PMID] [PMCID]

20. Okur EE, Akdaşçi E, Eker F, Bechelany M , Karav S. Silver nanoparticles as anticancer agents: mechanisms insight, current studies, and limitations. Pharmaceuticals.2026 19(2): 241 . [DOI:10.3390/ph19020241] [PMID] [PMCID]

21. Siquan L, Weilin C, Xiuwen C, Meiyan Z, Weihong G, Xiaoli F. Evaluating the safety and efficiency of nanomaterials: A focus on mitochondrial health. Biomed Pharmacother.2024; 180: 117484.

[DOI:10.1016/j.biopha.2024.117484] [PMID]

22. Xiong H, Nie X, Cao W, Zhu J, Chen J, Liu R,et al. Investigation of mitochondria-dependent apoptosis pathway and lipid peroxidation level induced by biosynthesized silver nanoparticles: Caspase-3 activation, BAK1/BCLx regulation and malondialdehyde production. Cancer Nanotechnology.2024;15(1): 13. [DOI:10.1186/s12645-024-00248-4]

23. Ahsan A, Gao GF, Tian WX. Phytogenic silver nanoparticles derived from Ricinus communis and Aloe barbadensis: synthesis, characterization, and evaluation of Biomedical Potential. Bioengineering.2025; 12(11);1273 [DOI:10.3390/bioengineering12111273] [PMID] [PMCID]

24. Brodzikowska A, Górski B, Michałowski K. Phytochemistry and application of white Mustard (Sinapis alba) in medicine and dentistry-A narrative review. Molecules.2026; 31(4). [DOI:10.3390/molecules31040674] [PMID] [PMCID]

25. Zubair H. Principles, techniques, and precautions in transwell migration and invasion assays for cancer cell metastasis research.protocol.io.2023; [DOI:10.17504/protocols.io.5qpvo3wn9v4o/v1]

26. Mustafa M, Ahmad R, Tantry IQ, Ahmad W, Siddiqui S, Alam M, et al. Apoptosis: a comprehensive overview of signaling pathways, morphological changes, and physiological significance and therapeutic implications.2024; Cells, 13(22): 1838

[DOI:10.3390/cells13221838] [PMID] [PMCID]

27. Ullah I, Khalil AT, Ali M, Iqbal J, Ali W, Alarifi S,et al.Green-synthesized silver nanoparticles induced apoptotic cell death in MCF-7 breast cancer cells by generating reactive oxygen species and activating caspase 3 and 9 enzyme activities. Oxid Med Cell Long.2020; 2020(1): 1215395. [DOI:10.1155/2020/1215395] [PMID] [PMCID]

28. Bandara S, Du H, Carson L, Bradford D, Kommalapati R. Agricultural and biomedical applications of chitosan-based nanomaterials. Nanomaterials.2020; 10(10): 1903. [DOI:10.3390/nano10101903] [PMID] [PMCID]

29. Wu Z, Hu Y, Hao R, Li R, Lu X, Itale M,et al. Research progress of genomics applications in secondary metabolites of medicinal plants: a case

study in safflower.2025; Int J Mol Sci. 26(8), 3867. [DOI:10.3390/ijms26083867] [PMID] [PMCID]

30. Janthong A, Utama K, Khamto N, Chawapun P, Siriphong S, Van Doan H,et al. Semi-synthetic flavonoid derivatives from Boesenbergia rotunda induce extrinsic apoptosis pathway via caspase-3 and caspase-8 in HCT116 colon cancer cell lines. Bioorgan Chem.2025; 159, 108343. [DOI:10.1016/j.bioorg.2025.108343] [PMID]

31. Pandey P, Lakhanpal S, Bishoyi AK, Jyothi SR, Mishra S, Verma M,et al. Biosynthesis of silver nanoparticles from plant extracts: a comprehensive review focused on anticancer therapy. Front Pharmacol.2025; 16:1600347. [DOI:10.3389/fphar.2025.1600347] [PMID] [PMCID]

32. Leiphrakpam PD, Are C. PI3K/Akt/mTOR signaling pathway as a target for colorectal cancer treatment. Int J Mol Sci.2024; 25(6): 3178. [DOI:10.3390/ijms25063178] [PMID] [PMCID]

33. Kumar A, Rai Y, Bhatt AN. Anti-cancer drug-mediated increase in mitochondrial mass limits the application of metabolic viability-based MTT assay in cytotoxicity screening. Cytotechnology.2024;76(3), 301-11. [DOI:10.1007/s10616-024-00618-1] [PMID] [PMCID]

34. Taherpour A, Zarban A, Asadian AH, Karbasi S, Shakibaie M. Efficacy of curcumin-synthesized silver nanoparticles on MCF-7 breast cancer cells. Med Oncol.2025; 42(7), 265. [DOI:10.1007/s12032-025-02809-y] [PMID]